Development 133, 4355-4365 (2006) doi:10.1242/dev.02624

Phosphorylation of IP_3R1 and the regulation of $[Ca^{2+}]_i$ responses at fertilization: a role for the MAP kinase pathway

Bora Lee[1,*], Elke Vermassen[2,*,†], Sook-Young Yoon[1], Veerle Vanderheyden[2], Junya Ito[1], Dominique Alfandari[1], Humbert De Smedt[2], Jan B. Parys[2] and Rafael A. Fissore[1,§]

A sperm-induced intracellular Ca^{2+} signal ($[Ca^{2+}]_i$) underlies the initiation of embryo development in most species studied to date. The inositol 1,4,5 trisphosphate receptor type 1 (IP_3R1) in mammals, or its homologue in other species, is thought to mediate the majority of this Ca^{2+} release. IP_3R1-mediated Ca^{2+} release is regulated during oocyte maturation such that it reaches maximal effectiveness at the time of fertilization, which, in mammalian eggs, occurs at the metaphase stage of the second meiosis (MII). Consistent with this, the $[Ca^{2+}]_i$ oscillations associated with fertilization in these species occur most prominently during the MII stage. In this study, we have examined the molecular underpinnings of IP_3R1 function in eggs. Using mouse and *Xenopus* eggs, we show that IP_3R1 is phosphorylated during both maturation and the first cell cycle at a MPM2-detectable epitope(s), which is known to be a target of kinases controlling the cell cycle. In vitro phosphorylation studies reveal that MAPK/ERK2, one of the M-phase kinases, phosphorylates IP_3R1 at at least one highly conserved site, and that its mutation abrogates IP_3R1 phosphorylation in this domain. Our studies also found that activation of the MAPK/ERK pathway is required for the IP_3R1 MPM2 reactivity observed in mouse eggs, and that eggs deprived of the MAPK/ERK pathway during maturation fail to mount normal $[Ca^{2+}]_i$ oscillations in response to agonists and show compromised IP_3R1 function. These findings identify IP_3R1 phosphorylation by M-phase kinases as a regulatory mechanism of IP_3R1 function in eggs that serves to optimize $[Ca^{2+}]_i$ release at fertilization.

KEY WORDS: Fertilization, Ca^{2+}, IP3R1, Mouse, MAPK, *Xenopus*

INTRODUCTION

In preparation for fertilization, ovulated mammalian eggs are arrested at the metaphase stage of the second meiosis (MII). Sperm entry triggers a series of increases in the intracellular free-Ca^{2+} concentration ($[Ca^{2+}]_i$), termed $[Ca^{2+}]_i$ oscillations, which enable exit from the MII arrest and induce egg activation (Miyazaki et al., 1993). Egg activation entails the orderly initiation of several events, including cortical granule exocytosis, extrusion of the second polar body (2PB), pronuclear (PN) formation and progression into interphase, the completion of which is required for the normal initiation of development (Ducibella et al., 2002; Schultz and Kopf, 1995).

Fertilization-associated $[Ca^{2+}]_i$ responses are known to involve stimulation of the phosphoinositide pathway, whereby a phospholipase C (PLC) enzyme hydrolyzes phosphatidylinositol 4,5-bisphosphate [PIP_2; PtdIns(4,5)P_2] to produce inositol 1,4,5-trisphosphate [IP_3; Ins(1,4,5)P_3] and diacylglycerol (DAG) (Halet et al., 2004; Stith et al., 1993; Turner et al., 1984). In mammals, a recently identified sperm-specific PLC isoform, PLCζ, is thought to represent the sperm factor responsible for the sustained $[Ca^{2+}]_i$ oscillations and production of IP_3 (Kouchi et al., 2004; Saunders et al., 2002). IP_3 promotes Ca^{2+} release by binding to the IP_3 receptors (IP_3Rs), which are predominantly located on the endoplasmic reticulum (ER) – the main reservoir of intracellular Ca^{2+} (Berridge, 2002; Berridge et al., 2000). IP_3Rs are thought to mediate all of the intracellular Ca^{2+} release required to induce egg activation (Miyazaki et al., 1992; Runft et al., 1999).

IP_3Rs are well suited to mediate the highly specialized spatiotemporal patterns of $[Ca^{2+}]_i$ responses that underlie fertilization. For example, IP_3Rs function as tetramers and each monomer consists of three functional domains: an N-terminal domain that contains the IP_3-binding site; a modulatory domain; and a C-terminal domain that includes the channel region of the molecule (Bezprozvanny, 2005; Bosanac et al., 2004; Patel et al., 1999). In addition, the entire sequence of IP_3Rs is lined with highly conserved consensus sites for interacting partner proteins that are likely to influence the properties of the receptor, such as affinity and/or conductivity (Patterson et al., 2004b), its location and distribution (Vermassen et al., 2004b).

Mammalian oocytes and eggs almost exclusively and abundantly express the type 1 IP_3R isoform (IP_3R1) (He et al., 1999; Parrington et al., 1998); oocytes of other vertebrates and invertebrates also express a single IP_3R isoform that is closely related to IP_3R1 (Iwasaki et al., 2002; Kume et al., 1993). The most conspicuous mode of regulation of IP_3R1 function in these cells is associated with maturation and cell-cycle transitions. For example, Ca^{2+} release through IP_3R1 is greatly enhanced after the initiation of oocyte maturation (Chiba et al., 1990; Fujiwara et al., 1993; Mehlmann and Kline, 1994) and, in vertebrate eggs, maximal IP_3R1-mediated Ca^{2+} release is closely timed to coincide with sperm entry, which takes place at one of the two M-phase stages of meiosis according to the species (Fujiwara et al., 1993; Kume et al., 1993; McDougall and Levasseur, 1998). Likewise, exit from M-phase and progression into interphase is associated with attenuation and cessation of the $[Ca^{2+}]_i$ responses (Jones et al., 1995; Parrington et al., 1998), which is accompanied by a pronounced loss of IP_3R1 function (FitzHarris et

[1]Molecular and Cellular Biology Program and Department of Veterinary and Animal Sciences, University of Massachusetts, Amherst, MA 01002, USA. [2]Laboratorium voor Fysiologie, Katholieke Universiteit Leuven, Campus Gasthuisberg O/N1, bus 802, B-3000 Leuven, Belgium.

*These authors contributed equally to this work
†Present address: Laboratorium voor Toxicologie en Bromatologie, Katholieke Universiteit Leuven, Campus Gasthuisberg O/N2, bus 922, B-3000 Leuven, Belgium
§Author for correspondence (e-mail: rfissore@vasci.umass.edu)

Accepted 31 August 2006

al., 2003; Jones and Whittingham, 1996). Given that during maturation and after activation/fertilization the changes in IP_3R1 concentrations and content of the Ca^{2+} stores are small (Brind et al., 2000; Iwasaki et al., 2002; Jellerette et al., 2000), it is likely that other mechanisms might regulate IP_3R1 function in eggs.

Phosphorylation has been shown to be an important regulatory mechanism of IP_3R1 function (Bezprozvanny, 2005; Patterson et al., 2004a). Among the protein kinases that phosphorylate IP_3R1 are: protein kinase A and protein kinase C (Ferris et al., 1991; Vermassen et al., 2004a); protein kinase G (Koga et al., 1994); Ca^{2+}/calmodulin-dependent protein kinase II (Ferris et al., 1991; Zhu et al., 1996); the tyrosine kinases Fyn (Jayaraman et al., 1996) and Lyn (Yokoyama et al., 2002); Rho kinase (Singleton and Bourguignon, 2002); and, very recently, protein kinase B (Khan et al., 2006) (V.V., H.D.S. and J.B.P., unpublished). In most cases, IP_3R1 phosphorylation by these kinases enhances Ca^{2+} conductivity, but none of these kinases appears to be intimately associated with cell-cycle transitions. Most importantly, abrogation of their activities by pharmacological inhibitors does not affect IP_3R1 function in eggs (Carroll and Swann, 1992; Smyth et al., 2002; Swann et al., 1989). However, a recent report has shown in vitro and in vivo IP_3R1 phosphorylation at several highly conserved consensus sites by Cdc2/cyclin B [also known as maturation promoting factor (MPF)], the kinase responsible for promoting resumption of meiosis and cell-cycle transitions (Malathi et al., 2003). Furthermore, Cdc2/cyclin B is, together with mitogen-activated protein kinase (MAPK), responsible for arresting vertebrate eggs at the MII stage (Masui and Markert, 1971). It is presently not known whether Cdc2/cyclin B phosphorylates IP_3R1 in oocytes and eggs, but our findings demonstrating cell-cycle stage-specific IP_3R1 phosphorylation in mouse eggs is in keeping with the hypothesis that receptor phosphorylation underlies, at least in part, the entrainment of the cell cycle with $[Ca^{2+}]_i$ responses in eggs and embryos (Jellerette et al., 2004). We detected IP_3R1 phosphorylation using the MPM2 antibody, which recognizes a large group of phospho-proteins active at mitosis (Davis et al., 1983; Westendorf et al., 1994). However, it is not known what kinase(s) is responsible for this phosphorylation, at which site(s) or domain(s) this modification takes place, or whether it affects the ability of mouse eggs to mount $[Ca^{2+}]_i$ oscillations.

In this study, we have analyzed IP_3R1 phosphorylation in oocytes, eggs and zygotes. We show that IP_3R1 MPM2 immunoreactivity is first detected during the early stages of oocyte maturation and decreases after fertilization, immediately preceding PN formation. We report the presence of a highly conserved MAPK phosphorylation consensus site within the IP_3-binding domain of IP_3R1 and show in vitro phosphorylation of this site by MAPK. Finally, we reveal that the MAPK signaling pathway is required for MPM2-detectable IP_3R1 phosphorylation in vivo and that abrogation of this pathway impairs the oscillatory activity of mouse eggs.

MATERIALS AND METHODS

Recovery of oocytes/eggs and culture conditions

Germinal vesicle (GV) oocytes and MII eggs were collected from the ovaries and oviducts of 6- to 8-week-old CD-1 female mice, respectively. Females were superstimulated with an injection of 5 IU PMSG (Sigma, St Louis, MO; all chemicals were from Sigma unless otherwise specified). GV oocytes were recovered 40 hours post-PMSG in HEPES-buffered Tyrode-Lactate solution (TL-HEPES) supplemented with 5% heat-treated fetal calf serum (FCS; Gibco, Grand Island, NY) and 100 μM 3-isobutyl-1-methylxanthine (IBMX). GV oocytes were matured for 12-16 hours in Chatot, Ziomek, and Bavister (CZB) medium (Chatot et al., 1989) containing 3 mg/ml bovine serum albumin (BSA) under paraffin oil at 36.5°C and in a humidified atmosphere containing 6% CO_2. In vivo MII eggs were recovered 12-14 hours after injection of 5 IU hCG, which was administered 45-48 hours after PMSG stimulation, and, after the removal of cumulus cells, were transferred into 50 μl drops of KSOM (Potassium Simplex Optimized Medium; Specialty Media, Phillipsburg, NJ) and cultured as above.

Parthenogenetic egg activation

The release of MII arrest and generation of zygotes was accomplished by exposing eggs to Ca^{2+}-free CZB medium supplemented with 10 mM $SrCl_2$ for 2 hours, as described by our laboratory (Jellerette et al., 2000). Activated eggs were transferred to drops of KSOM, cultured as above, and monitored for signs of activation, such as 2PB extrusion and PN formation.

Microinjection of eggs and preparation of PLCζ mRNA

Eggs were microinjected as previously described (Kurokawa et al., 2004). Reagents were diluted in injection buffer [100 mM KCl and 10 mM HEPES (pH 7.0)], loaded into glass micropipettes and delivered by pneumatic pressure (PLI-100 picoinjector, Harvard Apparatus, Cambridge, MA). Each egg received 7-12 pl (~1-3% of the total volume of the egg). pBluescript containing the full-length coding sequence of mouse PLCζ (a gift from Dr K. Fukami, Tokyo University of Pharmacy and Life Science, Japan) downstream of a T7 promoter was in vitro transcribed using the T7 mMESSAGE mMACHINE Kit (Ambion, Austin, TX), as reported by us (Kurokawa et al., 2004).

Fluorescence recordings and $[Ca^{2+}]_i$ determinations

Measurements of $[Ca^{2+}]_i$ were performed using Fura2AM (Molecular Probes, Eugene, OR) as previously reported by our laboratory (Kurokawa et al., 2005). Eggs were monitored in drops of TL-HEPES under mineral oil. Up to ten eggs were monitored simultaneously using the software SimplePCI (C-Imaging System, Cranberry Township, PA), which controls a high-speed filter wheel rotating between excitation wavelengths of 340 and 380 nm. Illumination was provided by a 75 W Xenon arc lamp and the emitted light above 510 nm was collected by a cooled Photometrics SenSys CCD camera (Roper Scientific, Tucson, AZ). Fluorescence ratios of 340/380 nm were obtained every 20-30 seconds.

Histone 1 (H1) and myelin basic protein (MBP) kinase assays and kinase inhibitors

The activities of MPF and MAPK in eggs and zygotes were assayed as described previously (Gordo et al., 2002). Lysates from five eggs were mixed in kinase buffer with a cocktail consisting of ATP, [γ-^{32}P]ATP (Amersham, Arlington Heights, IL), H1 (as a substrate for MPF) and MBP (as a substrate for MAPK). The reaction was allowed to proceed for 30 minutes at room temperature and was terminated by the addition of an equal volume of 2×Laemmli sample buffer (SB) (Laemmli, 1970). Proteins were separated on 15% SDS-polyacrylamide gels, and H1 and MBP phosphorylations visualized by autoradiography. Autoradiographs were scanned and quantified as described for western blotting.

U0126 (Calbiochem, San Diego, CA), a MEK-specific inhibitor, was prepared in dimethyl sulfoxide (DMSO) and routinely used at 25 μM; the inactive analog U0124 was used as a negative control. Roscovitine (Ros; Calbiochem), an inhibitor of Cdk1 and Cdk2, was prepared in DMSO and used at 75 μM for all experiments.

Antibodies

Immunological detection of IP_3R1 was carried out using the Rbt03 polyclonal antibody raised against C-terminal amino acids 2735-2749 of mouse IP_3R1 (Parys et al., 1995). For detection of IP_3R1 and IP_3R3, the pan-specific antibody Rbt475 was used, the epitope of which (amino acids 127-141 of mouse IP_3R1) is conserved between isoforms and across species (Bultynck et al., 2004). The anti-cytI3b-1 antibody, which has amino acids 378-450 as its epitope (Sipma et al., 1999), was used to identify the GST-fusion protein containing domain 2 (amino acids 346-922) of IP_3R1. The MPM2 monoclonal antibody (Upstate, Lake Placid, NY), which recognizes an epitope characterized by a phosphorylated serine (S)/threonine (T) followed by a proline (P) residue, and the 16B4 monoclonal antibody (Alexis

Biochemicals, Lausen, Switzerland), which recognizes a phosphorylated S followed by either a P or a K residue, were used to ascertain IP_3R1 phosphorylation.

Preparation of *Xenopus* eggs/zygotes lysates and IP_3R1 immunoprecipitation

Xenopus eggs were collected from mature females and in vitro fertilized, as per standard protocols. For immunoprecipitation experiments, groups of 25 unfertilized eggs or eggs collected after insemination were frozen on dry ice and solubilized with 500 μl cold embryo solubilization buffer containing 1.0% Triton X-100 (Cousin et al., 2000). Cellular debris was pelleted by centrifugation at 4°C and discarded. Supernatants were incubated overnight at 4°C with preimmune serum, Rbt03 antibody or MPM2 antibody, with head-over-head rotation. Incubation of protein A sepharose beads (Amersham) with the immunocomplexes occurred for an additional 3 hours before several washes with PBS. Samples were denatured by the addition of 2×SB and stored at –80°C until western blotting was performed.

Western blotting

Cell lysates from 15 to 100 mouse eggs or 0.5 to 6.0 *Xenopus* eggs were mixed with 15 μl of 2×SB, boiled and loaded onto NuPAGE Novex 3-8% Tris-Acetate gels (Invitrogen, Carlsbad, CA). After electrophoresis, proteins were transferred onto nitrocellulose membranes (Micron Separations, Westboro, MA). Successive MPM2 and IP_3R1 western blotting were performed as described by our laboratory (Jellerette et al., 2004). Membranes were washed and incubated for 1 minute in chemiluminescence reagent (NEN Life Science Products, Boston, MA) and developed according to the manufacturer's instructions. Each nitrocellulose membrane was digitally captured and quantified using an imaging system (Kodak Imaging Station 440 CF, Rochester, NY); quantification was performed in the TIFF files before any rendering was carried out. The intensity of the MPM2 immunoreactive band (also the phosphorylated substrate bands in kinase assays) from MII eggs was arbitrarily given the value of 1 and values in other lanes were expressed relative to this band from MII eggs. Intensities were plotted using Sigma Plot (Jandel Scientific Software, San Rafael, CA). Figures were prepared from the TIFF files using ImageJ software (NIH; http://rsb.info.nih.gov/ij/) and Microsoft Powerpoint.

IP_3R1 GST constructs and mutagenesis

For domain analysis we expressed GST-fusion proteins corresponding to the various IP_3R1 domains that can be obtained by limited proteolysis (Yoshikawa et al., 1999). The cDNAs encoding domains 1-6 of mouse IP_3R1 were amplified by PCR using the full-length mouse IP_3R1 cDNA as a template (a kind gift from Dr K. Mikoshiba, Tokyo, Japan) and the primers listed in Table 1. Purified PCR products were ligated into the pGEX-6p2 vector and transformed into *E. coli* DH5α or Bl21 (DE3). Site-directed mutagenesis was performed using the Quick-Change point-mutation kit (Stratagene, La Jolla, CA, USA). Forward primers were designed according to the manufacturer's recommendation and reverse primers were the complementary sequence of the forward primers. Single mutations were made using pGEX6p2-IP_3R1 domain 2 as a template, whereas the double mutation was made using pGEX6p2-IP_3R1 domain 2 S421A as template cDNA. GST-fusion proteins were purified as previously described (Bultynck et al., 2001). All constructs were sequenced to confirm mutations and frame.

In vitro phosphorylation of IP_3R1 by ERK/MAPK

GST-IP_3R1 fragments (0.5 μg) were diluted in phosphorylation buffer supplemented with 30 μM ATP and 20 μCi [γ-^{32}P]ATP (Vermassen et al., 2004a). Full-length mouse IP_3R1 and full-length rat IP_3R3 (1 μg) were expressed in Sf9 insect cells, purified and diluted in phosphorylation buffer supplemented with 0.18% CHAPS and 0.072% L-α-phosphatidylcholine, as previously described (Vermassen et al., 2004a). Free Ca^{2+} concentrations in in vitro phosphorylation reactions (40 μM Ca^{2+}) were calculated using the CaBuf software (Dr G. Droogmans, K.U. Leuven, Belgium; available at ftp://ftp.cc.kuleuven.ac.be/pub/droogmans/). Reactions were performed at 30°C for 1 hour and initiated by the addition of 250 ng (GST-IP_3R1 fragments) or 400 ng (IP_3R1 and IP_3R3) of the activated ERK2 kinase (Calbiochem). Reactions were stopped by heating the samples for 10 minutes at 70°C in 2×SB. Incorporation of ^{32}P was determined using the Storm 840 PhosphorImager (Molecular Dynamics, Sunnyvale, CA), as previously reported (Vermassen et al., 2004a).

Statistical analysis

Values from three or more experiments, performed on different batches of eggs or zygotes, were used for the evaluation of statistical significance. Statistical comparisons of the intensity of IP_3R1 bands, kinase assays and $[Ca^{2+}]_i$ parameters were performed using the Student's *t*-test or one-way ANOVA and, if differences were observed between groups, comparisons between treatments were carried out by applying the Tukey/Kramer test using the JMP-IN software (SAS Institute, Cary, NC). Differences were considered to be significant when $P<0.05$. Significance among groups/treatments is denoted in bar graphs by different superscripts (western blots) or by the presence of one or two asterisks (kinase assays).

RESULTS

IP_3R1 is differentially phosphorylated in mouse oocytes, eggs and zygotes

Our previous study demonstrated that IP_3R1 is phosphorylated in a M-phase stage-specific manner in mouse eggs and interphase zygotes (Jellerette et al., 2004). In the present investigation, we sought to extend those findings by examining IP_3R1 MPM2 reactivity in mouse oocytes during maturation and in zygotes throughout the first cell cycle. Western blotting was performed on lysates of oocytes at the GV stage (0 hours of maturation), at the onset of germinal vesicle breakdown (GVBD; 2 hours), at meiosis I (MI; 8 hours) and at MII (IVM/MII; 12 hours). MPM2 immunoreactivity of a protein of ~270 kDa molecular mass corresponding to the IP_3R1 (Jellerette et al., 2004) was nearly undetectable at the GV stage, but showed a dramatic increase at

Table 1. Forward (F) and reverse (R) primers used to synthesize IP_3R1 GST-fusion proteins

Primer name	5′ restriction site	Sequence 5′-3′
Domain 1F	*Bam*HI	ACTAAAGGATCCATGTCTGACAAAATGTCG
Domain 1R	*Eco*RI	CAAGGAATTCCC**TAG**TCTCAACCTACTCCGAGA
Domain 2F	*Bam*HI	ACTAAAGGATCCAACGCGCAAGAAAAAATG
Domain 2R	*Eco*RI	CAAGGAATTCCC**TAG**CCTCATCACGTTACTGCC
Domain 3F	*Eco*RI	GACGGAATTCCCTCTATCCATGGCGTTGGG
Domain 3R	*Xho*I	CAAGCTCGAGCG**TAG**TCGGGCTGATAACCGCCA
Domain 4F	*Bam*HI	ACTAAAGGATCCAACGCCGCTCGCAGAGAC
Domain 4R	*Eco*RI	CAAGGAATTCCC**TAG**CCTCCGGAAGGTGGTAAA
Domain 5F	*Xho*I	GACACTCGAGCGGAGGCCGACCCTGATGAC
Domain 5R	*Not*I	AACGCGGCCGCA**TAG**GTCGATGATGACCCCGAA
Domain 6F	*Bam*HI	ACTAAAGGATCCACCTTTGCTGACCTGAGG
Domain 6R	*Eco*RI	CAAGGAATTCCC**TAG**GGCCCGGCTGCTGTGGGTT

Restriction sites are underlined and the stop codons are indicated in bold.

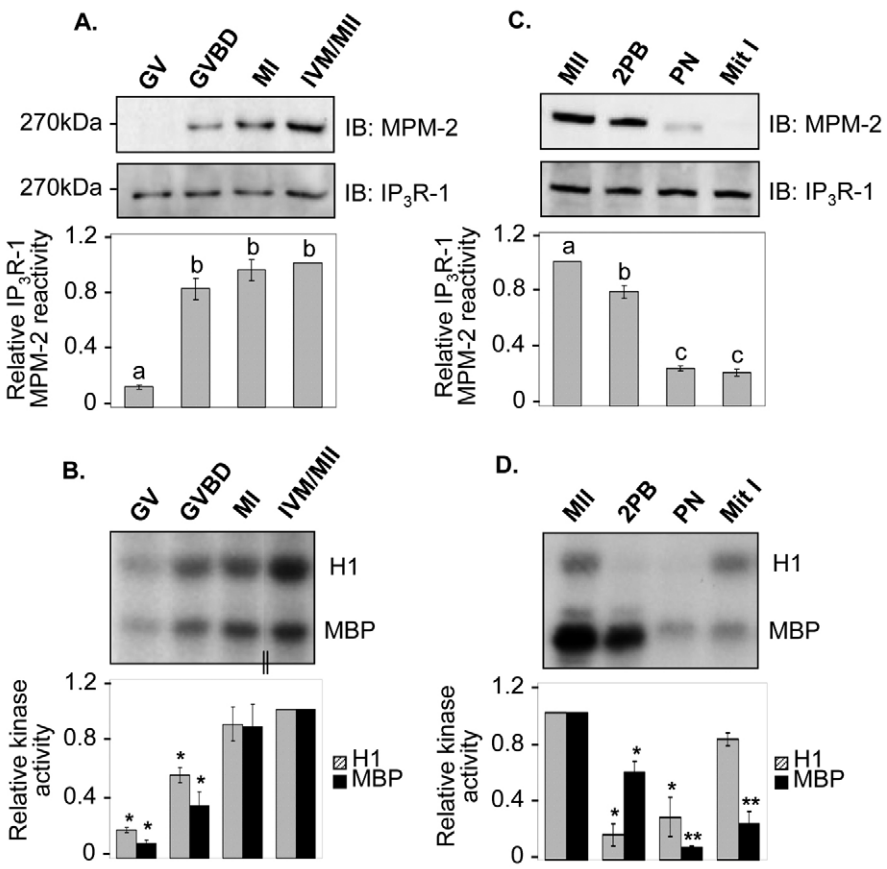

Fig. 1. IP_3R1 is differentially phosphorylated in mouse oocytes, eggs and zygotes. (**A**) Immunoblots (IB) of oocyte lysates during different stages of oocyte maturation (GV, GVBD, MI and IVM/MII) were probed with the MPM2 antibody (upper panel) and, after stripping of the blot, with the IP_3R1 antibody (lower panel). Quantification of IP_3R1 MPM2 reactivity is shown in the graph below the IB panels. Data are presented as means±s.e.m., both here and throughout the manuscript. Fifty mouse oocytes were used per lane, both here and elsewhere in the study. (**B**) Kinase activity assays performed on lysates from five oocytes collected simultaneously with oocytes for western blotting; H1 and MBP phosphorylation indicate MPF and MAPK activity, respectively. The graph below shows quantification of kinase activities. Bars with an asterisk are significantly different from those without a symbol within kinase here and elsewhere. The presence of two vertical lines indicates that lanes were cut and pasted from the same blot/exposure during the preparation of the figure here and elsewhere in the manuscript. (**C**) Lysates from MII eggs and zygotes collected at 2PB, PN and Mit I were probed with MPM2 antibody (upper panel) and re-probed with IP_3R1 antibody (lower panel), as described above. (**D**) Kinase activity assays performed at the same cell-cycle stages as for C. Bars with asterisks are significantly different from those without a symbol.

GVBD and reached near maximal reactivity at MI. This reactivity remained unchanged until MII (Fig. 1A, upper panel and bar graph). The changes in MPM2 reactivity were not due to changes in IP_3R1 mass during the same period of time, as stripping of the same blots followed by re-probing with an anti-IP_3R1 antibody revealed no such changes in the IP_3R1 signal (Fig. 1A, lower panel). Examination of MPF and MAPK activity using an in vitro kinase assay revealed that, consistent with the notion that MPM2 reactivity is associated with M-phase kinase activity, both MPF and MAPK were at basal levels at the GV stage but their activity had increased by the time of GVBD and was at near peak levels at both MI and MII stages (Fig. 1B).

We next examined IP_3R1 MPM2 immunoreactivity during the first cell cycle. Exit from MII arrest was induced by exposure to $SrCl_2$ (Kline and Kline, 1992a). Samples were collected at the time of 2PB release (2 hours after activation), at PN formation (6 hours post-activation, the time at which zygotes had reached interphase) and at first mitosis (Mit I), the beginning of which was noted by the breakdown of the PN envelope (PNBD; ~17 hours post-activation). Surprisingly, despite exit from MII as evidenced by the release of the 2PB, IP_3R1 MPM2 immunoreactivity was nearly unchanged 2 hours after activation (Fig. 1C). Conversely, a dramatic reduction of MPM2 reactivity took place as zygotes reached interphase and remained low until the time of Mit I (Fig. 1C, upper panel and bar graph); in three out of five replicates, MPM2 reactivity became nearly undetectable at Mit I. The overlapping IP_3R1 reactivity remained unchanged in $SrCl_2$-activated zygotes (Fig. 1C, lower panel). Concomitant evaluation of MPF and MAPK activities in these zygotes revealed the expected rapid inactivation of MPF and protracted loss of MAPK activity during the transition into interphase (Fig. 1D), and the increase in MPF activity, which occurred without a concurrent increase in MAPK activity, as zygotes gained entry into Mit I (Fig. 1D). Altogether, these results show that although IP_3R1 acquisition of MPM2 reactivity coincides with the increase of both MPF and MAPK activities during oocyte maturation, the presence and loss of this reactivity during the zygotic cell cycle are more closely associated with MAPK than with MPF.

IP_3R1 is differentially phosphorylated in *Xenopus* eggs and zygotes

To extend our findings to other species, and taking into account that cycling *Xenopus* egg extracts also show cell cycle-restricted $[Ca^{2+}]_i$ responses (Tokmakov et al., 2001), we examined whether IP_3R1 phosphorylation in *Xenopus* eggs exhibited the same association with the cell cycle. *Xenopus* egg extracts were prepared from unfertilized eggs and from fertilized eggs ~60 minutes after fertilization, which represented the MII and interphase stages, respectively. The results show that in *Xenopus* eggs, IP_3R1 also undergoes cell cycle-associated phosphorylation, as MPM2 reactivity was observed only in MII extracts (Fig. 2A, upper panel). Once again, IP_3R1 immunoreactivity was unchanged (Fig. 2A, lower panel).

To ascertain whether the band of ~270 kDa recognized by the MPM2 antibody was IP_3R1, we performed immunoprecipitation studies using either anti-IP_3R1 or MPM2 antibodies followed by blotting with the reciprocal antibody. These experiments were performed with *Xenopus* egg extracts, as they provide an abundant source of material (Parys et al., 1992). Probing of the material precipitated by either of the antibodies with the alternate antibody

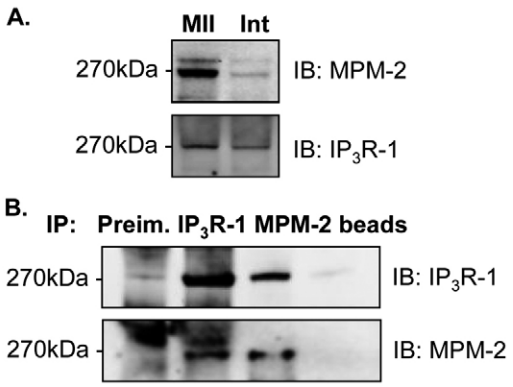

Fig. 2. IP_3R1 is differentially phosphorylated in *Xenopus* eggs and zygotes. (**A**) Western blotting performed on *Xenopus* egg extracts (approximately three eggs/lane) collected at MII and at interphase (Int) shows MPM2 (upper panel) and IP_3R1 reactivity (lower panel). (**B**) Immunoprecipitation (IP) experiments performed on MII *Xenopus* egg extracts using preimmune serum (Preim.), anti-IP_3R1 antibody, MPM2 antibody or beads alone, followed by SDS-PAGE and western blotting with the anti-IP_3R1 antibody (upper panel) and the MPM2 antibody (lower panel).

recognized a strong immunoreactive band, consistent with the notion that the ~270 kDa MPM2 immunoreactive band is IP_3R1 (Fig. 2B, upper panel, IP_3R1 blotting; lower panel, MPM2 blotting). Immunoprecipitation with pre-immune serum or beads alone produced negative results. Together, these results demonstrate that IP_3R1 in eggs is phosphorylated at a MPM2 consensus site(s) in a M-phase-specific manner.

M-phase kinase phosphorylation motifs in IP_3R1

The MPM2 antibody recognizes more than 50 proteins phosphorylated during the M-phase of the cell cycle (Westendorf et al., 1994). Remarkably, although the identity of the majority of proteins phosphorylated at the MPM2 epitope is known, that of the kinases responsible for most of these phosphorylations is not (Che et al., 1997). Likewise, the kinase(s) responsible for MPM2 IP_3R1 phosphorylation also remains to be identified. The preferred MPM2 epitope sequence reportedly consists of a hydrophobic amino acid-phosphoserine or phosphothreonine-proline-hydrophobic amino acid or an uncharged amino acid (Che et al., 1997; Ding et al., 1997). Given that MPM2 kinases are likely to be proline-targeted kinases and that the S/T-P motif coincides with the minimal phosphorylation motif for Cdc2/cyclin B and MAPK, we examined the presence of phosphorylation motifs for these kinases in IP_3R1 using an 'in-silico' approach. In a recent manuscript, the presence of two highly conserved Cdc2/cyclin B consensus sites centered on amino acids S^{421} and T^{799}, which lie in the consensus motif S/T-P-X-K/R (Nigg, 1991), of IP_3R1 has been reported (Malathi et al., 2003). Whereas S^{421} was restricted to IP_3R1, T^{799} was also present in IP_3R3 (Malathi et al., 2003). Here, we report that IP_3R1 also contains two conserved consensus sequences for MAPK/ERK phosphorylation: P-X-S/T-P (Che et al., 1997), which are centered on S^{436} and T^{945}, respectively. S^{436} is conserved in IP_3R1 from mouse to *Drosophila*, whereas T^{945} is conserved only among IP_3R1 in vertebrates (Fig. 3). A third site, centered on S^{1765}, is present, but only in the IP_3R1 of some vertebrates, such as mouse, rat and bovine, but not in human or in *Xenopus*. None of these sites is conserved in IP_3R2 or IP_3R3 (Fig. 3).

IP_3R	S^{436}	T^{945}	S^{1765}
Mouse-1	iv**pvsp**ae	fl**pmtp**ma	ng**plsp**gg
Human-1	iv**pvsp**ae	fl**pmtp**ma	ng**plsa**gg
Bovine-1	iv**pvsp**ae	fl**pmtp**ta	ng**plsp**gg
Rat-1	iv**pvsp**ae	fl**pmtp**ma	ng**plsp**gg
Xenopus	iv**pvsp**ae	fl**pmtp**ma	ng**plsg**gs
Drosophila	li**pvsp**ve	oa**iaap**ti	aa**plmd**pa
Mouse-2	iv**cvpl**se	If**pvsv**pd	ng**plsg**ay
Human-2	iv**svpl**se	if**pmsv**pd	ng**hlsg**ay
Mouse-3	sv**pvse**ir	sv**fgas**sl	sg**ldqd**ws
Human-3	sv**pvse**ir	sv**fsap**sl	tg**ldpd**ws

Fig. 3. MAPK phosphorylation motifs are present in the sequence of IP_3Rs. The sequences of IP_3R1, IP_3R2 and IP_3R3 of various species were examined for the presence of MAPK sites. Two highly conserved (S^{436} and T^{945}) and one less conserved (S^{1765}) MAPK consensus sites were found in IP_3R1, but not in IP_3R2 or IP_3R3.

In vitro phosphorylation of IP_3R1 by MAPK

Whereas cellular MPM2 epitopes have been shown to be phosphorylated by both Cdc2/cyclin B and MAPK/ERK, in vitro phosphorylation studies using *Xenopus* egg extracts and a 19-residue peptide containing two representative MPM2 epitopes as a substrate, one of which closely matched the IP_3R1 S^{421}PLK motif, showed that the MPM2 phosphorylating activity of these extracts could be attributed almost exclusively to MAPK (Che et al., 1997; Kuang and Ashorn, 1993). Che et al. also showed that MPM2 epitope recognition by the antibody was enhanced by the presence of a proline residue near the N-terminal end of the MPM2 epitope (Che et al., 1997). Given that PVS^{436}P and PMT^{945}P are highly conserved in IP_3R1 and that they both have a proline residue at the –2 position, which renders them stronger MAPK consensus sites, we focused our in vitro IP_3R1 phosphorylation studies on this kinase. We first performed in vitro phosphorylation of the full-length IP_3R1 and –3 proteins that were expressed and purified from Sf9 insect cells in the presence of [γ-^{32}P] ATP. In vitro phosphorylation of IP_3Rs by activated ERK2 showed that, whereas IP_3R1 is an adequate substrate for the kinase, IP_3R3 is not (Fig. 4A). This finding is consistent with the absence of MAPK motifs in IP_3R3. Similar results were obtained with both of the monoclonal antibodies 16B4 and MPM2 (not shown). Equal loading of the proteins was confirmed by western blotting of the same membrane using the Rbt475 pan-IP_3R antibody (Fig. 4B).

To gain insight into the possible ERK phosphorylation sites on IP_3R1, in vitro assays were performed as above, but using GST-fusion proteins of large domains of the IP_3R1 that corresponded to the IP_3R1 fragments that can be generated in vitro by limited trypsinolysis (Yoshikawa et al., 1999). The cDNA constructs were generated by PCR and together encompassed the complete IP_3R1 coding sequence (except for the transmembrane regions; see Table 2). The results show that domains 2 and 4, both of which contain optimal consensus sequences for MAPK phosphorylation, were most strongly phosphorylated by ERK2 (Fig. 4C). Although a higher relative phosphorylation level was observed in domain 4, it is important to realize that the only potential MAPK-phosphorylation site in this domain, S^{1765}, is not conserved between mammals. For that reason, domain 4 was not investigated further.

Instead, we focused on GST-IP_3R1 domain 2, as it contained the most highly conserved site for MAPK phosphorylation (PVS^{436}P). Moreover, it is known that MPM2 reactivity is enhanced by the

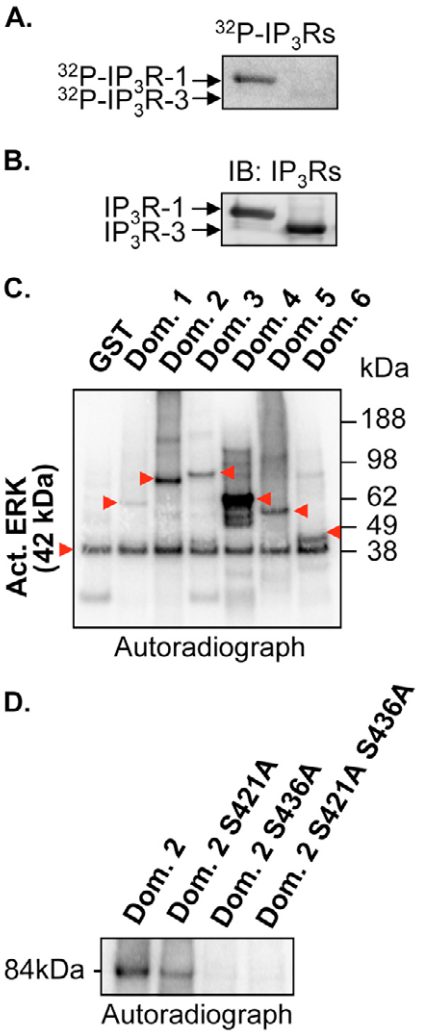

Fig. 4. In vitro phosphorylation of IP_3R1 and GST-IP_3R1 fragments by activated ERK2 kinase. (**A**) Purified IP_3R1 and IP_3R3 (1 μg) or GST-IP_3R1 purified fragments (0.5 μg) were phosphorylated in vitro in the presence of [γ-^{32}P]ATP at 30°C using activated ERK2. Phosphorylated IP_3Rs and GST-fusion fragments were detected using a phosphorimager. (**B**) Equal amounts of IP_3Rs in reaction were determined with an anti-IP_3R antibody that recognizes both isoforms equally. (**C**) Phosphorylation of IP_3R1 domains expressed as GST-fusion proteins by MAPK/ERK2 performed and quantified as above. Arrowheads indicate the position of ERK2 and of the various GST-fusion proteins. The amino acids included within each of the domains and the predicted molecular weight for each domain are noted in Table 2. (**D**) ERK2 phosphorylation of IP_3R1 domain 2 after in vitro mutagenesis of S^{421} and S^{436}. Equal loading was ascertained using the anti-cytI3b1 antibody (data not shown). All results are typical of at least three experiments.

presence of consensus sites in close succession and that S^{436} is preceded by a phosphorylation consensus site for Cdc2/cyclin B (S^{421}PLK) (Westendorf et al., 1994). We therefore chose to introduce inactivating mutations by site-directed mutagenesis of S^{421} (S→A) and S^{436} (S→A) to examine whether or not any of these sites was phosphorylated in vitro by MAPK. The results show that although the S^{421}→A mutation decreased overall phosphorylation of the domain, the S^{436}→A mutation completely abrogated phosphorylation of domain 2 by ERK2 (Fig. 4D). Together, these results show that at least one of the predicted MAPK/ERK sites within IP_3R1 is phosphorylated by the kinase during in vitro phosphorylation.

Table 2. Corresponding base pair numbers, number of amino acids and predicted molecular weight of each of the GST-fusion IP_3R1 fragments used for in vitro phosphorylation studies

Domain	Basepairs (pcDNA3.1-IP_3R1)	Amino acids	Molecular weight (kDa)
1	912-1946	1-345	61.0
2	1947-3677	346-922	83.7
3	3678-5654	923-1581	92.0
4	5655-6704	1582-1931	61.0
5	6705-7560	1932-2216	55.2
6	8682-9159	2590-2762	44.0

MAPK activity is required for MPM2 IP_3R1 phosphorylation of mouse eggs

Next, we examined whether MAPK/ERK2 was required for the MPM2-detectable phosphorylation of IP_3R1 observed in mouse eggs. Accordingly, to prevent ERK activity in oocytes, we used U0126, a specific pharmacological inhibitor of MEK1 and MEK2, the upstream kinases required for phosphorylation and activation of ERK (Favata et al., 1998). Exposure of the oocytes and eggs of several species to U0126 has already been shown to specifically block activation of the ERK pathway (Philipova et al., 2005; Phillips et al., 2002). In mouse eggs, this exposure produced cellular phenotypes consistent with the abrogation of this pathway by genetic methods (Colledge et al., 1994; Hashimoto et al., 1994). In our studies, oocytes were exposed to 25 μM U0126 or 25 μM U0124 (its inactive analog) prior to and during maturation. Because it is well established that oocytes matured in the absence of MAPK activity, as is the case here, either do not reach MII or progress into a MIII arrest (Araki et al., 1996), maturation was performed in the presence of colcemid, a microtubule disruptor that prevents exit from metaphase (Winston et al., 1995). After maturation, oocytes were examined for MPM2 and IP_3R1 immunoreactivity, and for in vitro kinase activity. Our results show that, whereas IP_3R1 in oocytes matured under control conditions acquired MPM2 reactivity, IP_3R1 reactivity at this epitope was precluded in oocytes matured in the presence of U0126 (Fig. 5A). Our data also show that U0126 induced the expected inactivation of MAPK activity, without diminishing MPF activity (Fig. 5B), which is consistent with our findings that U1026 affected neither the rate nor the timing of oocyte maturation (not shown).

Given the above results, we next determined whether untimely activation of MAPK could induce IP_3R1 MPM2 reactivity. As the low levels of IP_3R1 MPM2 reactivity at the time of PN formation coincide with basal levels of MPF and MAPK activities, we sought to increase MAPK activity at this stage by exposing zygotes to okadaic acid (OA). OA has been shown to induce precocious activation of MAPK and PNBD in mouse zygotes by inhibiting protein phosphatases PP1 and PP2A (Gordo et al., 2002; Moos et al., 1995). Treatment of PN zygotes with 10 μM OA for 60 minutes resulted in a sharp increase of IP_3R1 MPM2 immunoreactivity (Fig. 5C). This increase was largely precluded by U0126, but not by roscovitine (Meijer et al., 1997) (Fig. 5C). As expected, OA treatment strongly increased the level of MAPK activity, and the increase was inhibited by U0126 (Fig. 5D). Collectively, these results

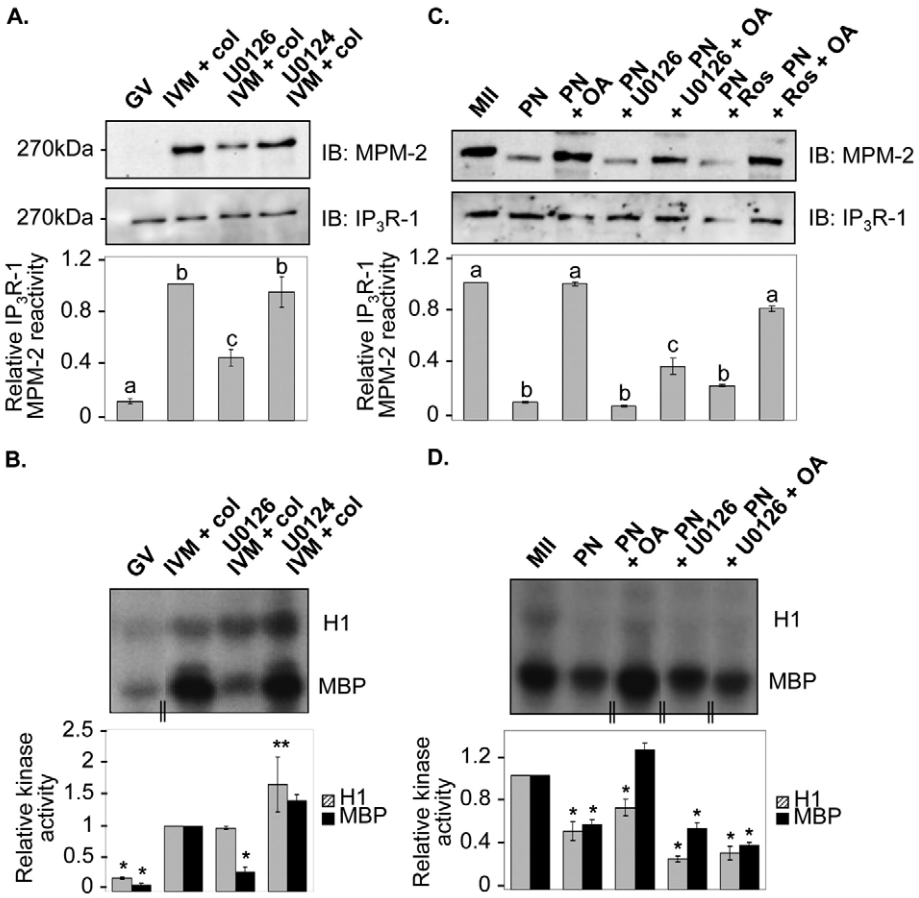

Fig. 5. MAPK activity is required for IP_3R1 MPM2 phosphorylation of mouse eggs. (**A**) IP_3R1 MPM2 (upper panel) and IP_3R1 (lower panel) reactivity in oocytes matured in vitro (IVM) in the presence of U0126 (25 μM), in its absence or in the presence of U0124. Quantification of IP_3R1 MPM2 reactivity is shown in the graph. (**B**) MPF and MAPK activities were assayed in the presence or absence of U0126 at the same time points as in A and are quantified in the graph below; asterisks indicate statistical significance. (**C**) IP_3R1 MPM2 (upper panel) and IP_3R1 (lower panel) reactivity in PN-stage zygotes treated with OA (10 μM), OA+U0126 (75 μM) or OA+roscovitine (Ros; 75 μM). The graph shows quantification of MPM2 reactivity. (**D**) Effect of OA on MPF and MAPK activities in PN-stage zygotes and inhibition of its effects by U0126 but not by Ros (not shown). The graph shows quantification of the effect of OA and U0126 on MPF and MAPK activities. Bars with asterisks are significantly different from those without a symbol.

demonstrate that the acquisition of MPM2 reactivity by IP_3R1 at MII and in PN zygotes requires elevated activity of MAPK, but not necessarily of MPF.

MPM2 IP_3R1 phosphorylation influences IP_3R1 function

We next investigated whether or not abrogation of MAPK activity and loss of MPM2 reactivity influenced the ability of eggs to initiate and maintain $[Ca^{2+}]_i$ oscillations. Accordingly, we matured oocytes as above in the presence of U0126 and colcemid and induced $[Ca^{2+}]_i$ oscillations 16 hours after initiation of maturation. First, we investigated the effects of U0126 on $SrCl_2$-induced oscillations. We reasoned that, as $SrCl_2$ promotes Ca^{2+} release via IP_3R1 without inducing IP_3 production (Brind et al., 2000; Jellerette et al., 2000), it would test IP_3R1 function in an independent way. In the second approach, we initiated physiological oscillations by injecting PLCζ mRNA, which induces oscillations by triggering IP_3 production (Saunders et al., 2002). Our results show that oocyte maturation in the presence of U0126 greatly reduced the ability of both activators to induce $[Ca^{2+}]_i$ oscillations. For example, although control oocytes mounted normal $[Ca^{2+}]_i$ oscillations in response to $SrCl_2$ stimulation (Fig. 6A, left panel), oscillations in U0126-treated eggs either terminated prematurely or were absent altogether (Fig. 6A, right panel). In addition, in the latter group, the observed rises were of lower amplitude and shorter duration, which is clearly evidenced in the side-by-side comparison of the parameters for the first $SrCl_2$-induced $[Ca^{2+}]_i$ rise between the control and U0126-treated eggs. For instance, the amplitude of the first rise, as assessed by the magnitude of the change in the fluorescence ratio of 340/380 nm (F340/F380), was of 1.5±0.06 for control eggs, whereas it was of 0.6±0.03 for U0126-treated eggs. Similarly, the duration of this rise was almost double for control eggs than for U0126-treated eggs (8.1±1.39 min versus 4.3±0.30 min, respectively). Likewise, oscillations initiated by injection of PLCζ mRNA terminated prematurely in U0126-treated oocytes and each of the $[Ca^{2+}]_i$ transients observed showed reduced amplitude and duration (Fig. 6B). For example, control eggs injected with 0.1 μg/μl PLCζ mRNA showed an average of 9.1±1.80 $[Ca^{2+}]_i$ rises in the first 2 hours of monitoring, whereas U0126-treated eggs only showed 1.3±0.45 rises in the same period of time. These effects cannot be attributed to inhibition of mRNA translation, as IP_3R1 degradation in these eggs was unaffected by U1026 (not shown).

Although the inhibition of $[Ca^{2+}]_i$ oscillations in those eggs by U0126 could strictly be due to the effects of abrogating MAPK activity on IP_3R1 function, the possibility cannot be excluded that, unrelated to IP_3R1 function, more extensive effects caused by the drug treatment could, at least in part, account for the cessation of oscillations. For example, the Ca^{2+} content of the stores or the Ca^{2+} influx required to refill these stores (also known as capacitative Ca^{2+} entry) could be compromised by lack of MAPK activity, thereby reducing the persistence of the oscillations. We first assessed whether the content of the intracellular Ca^{2+} stores was affected by maturation in the presence of U0126. To do this, eggs were treated with thapsigargin, a specific inhibitor of the sarcoplasmic/ER Ca^{2+} ATPase pumps (Thastrup et al., 1990) that has been widely used to estimate the Ca^{2+} content of IP_3-sensitive stores (Shuttleworth and Thompson, 1992; Kline and Kline, 1992b). In vitro oocyte maturation was performed as above in the presence of U0126 and

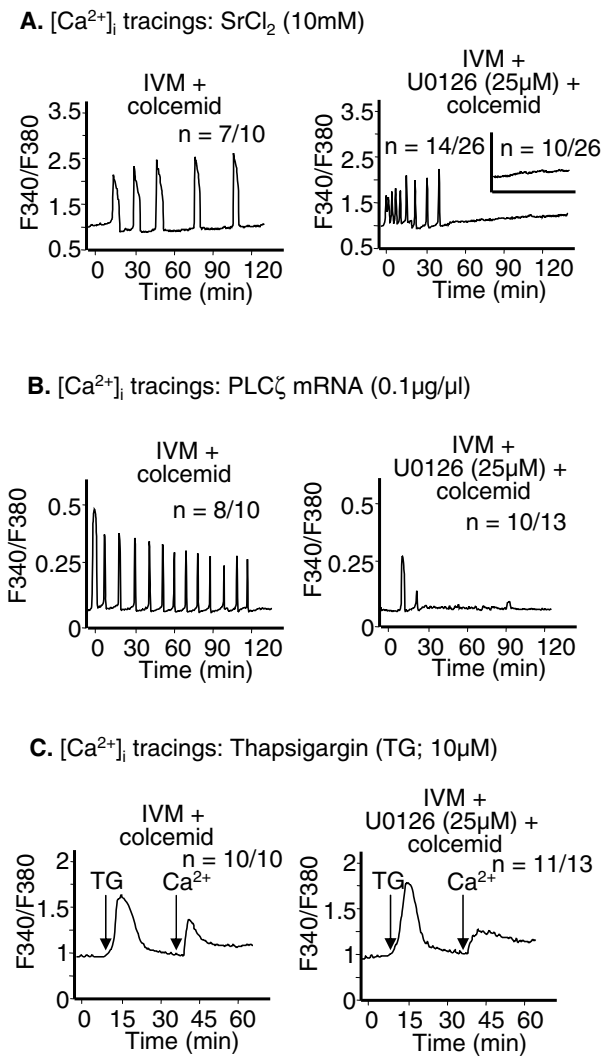

Fig. 6. Absence of MAPK activity and IP_3R1 MPM2 phosphorylation influences the ability of mouse eggs to mount oscillations and affects IP_3R1 function. (**A**) $[Ca^{2+}]_i$ responses induced by $SrCl_2$ (10 mM) and (**B**) PLCζ (0.1 μg/μl) were compared in oocytes matured in the absence (left panels) or presence (right panels) of U0126 (25 μM). (**C**) The content of the Ca^{2+} stores was examined in oocytes maturated in the absence (left panel) or presence of U0126 (right panel) by monitoring $[Ca^{2+}]_i$ responses induced by the addition of thapsigargin (first arrow; TG; 10 μM) in Ca^{2+}-free media. Ca^{2+} influx was examined in the same oocytes after the addition of $CaCl_2$ up to a final concentration of 5 mM (second arrow).

colcemid. After 14-16 hours, eggs were placed in medium devoid of external Ca^{2+} for 30 minutes, after which they were treated with 10 μM thapsigargin. The presence of U0126 did not affect the $[Ca^{2+}]_i$ responses elicited by thapsigargin (Fig. 6C), as the mean change in the F340/F380 ratio was of 0.7±0.16 for control eggs and of 0.7±0.14 for U0126-treated eggs. To investigate the effect of reduced MAPK activity during maturation on capacitative Ca^{2+} entry, we examined whether the increase in $[Ca^{2+}]_i$ elicited by the addition of $CaCl_2$ to the extracellular medium after thapsigargin treatment was affected. We found that Ca^{2+} influx into these eggs was not influenced by maturation in the presence of U0126 (Fig. 6C), as evidenced by the similarity in the mean change in the F340/F380 ratio between the control and U0126-treated eggs (0.30±0.13 versus 0.30±0.19, respectively). Collectively, our results are consistent with the model that the MAPK pathway is involved in the regulation of IP_3R1 function in eggs.

DISCUSSION

We have examined whether IP_3R1 phosphorylation at the MPM2 epitope, an epitope commonly phosphorylated by M-phase kinases, may underpin the enhanced functional activity of IP_3R1 in MII eggs. Our results show that MPM2 IP_3R1 phosphorylation is associated with the presence of $[Ca^{2+}]_i$ oscillations in mouse eggs and zygotes. Using in vitro assays, we found that MAPK/ERK2 phosphorylates IP_3R1 at a conserved consensus site and that MAPK activity is required for in vivo MPM2-detectable IP_3R1 phosphorylation. We also observed that abrogation of MPM2 IP_3R1 phosphorylation during maturation coincides with the failure of eggs to mount $[Ca^{2+}]_i$ oscillations. These results establish an unmistakable molecular link between the cell cycle and the Ca^{2+} releasing machinery.

The role of Ca^{2+} at fertilization represents, perhaps, the clearest manifestation of cell-cycle regulation by a second messenger, as a sperm-induced Ca^{2+} response is required to induce cell-cycle progression in all species studied to date (Stricker, 1999; Whitaker and Patel, 1990). An important feature of Ca^{2+} release during fertilization is that it almost universally unfolds during M-phase stages of the cell cycle (Stricker, 1999; Whitaker, 2006) and that, in those species in which the sperm initiates oscillations, attenuation of $[Ca^{2+}]_i$ oscillations coincides with transition into the interphase stages (Kono et al., 1996; McDougall and Levasseur, 1998; Stricker and Smythe, 2003). Appropriately, both IP_3R1 function, as examined by IP_3-induced Ca^{2+} release, and IP_3R1 cellular distribution, especially its reorganization into cortical clusters, coincide with these highly oscillatory M-phase stages (FitzHarris et al., 2003; Goud et al., 1999; Jellerette et al., 2004; Kline et al., 1999; Parrington et al., 1998). However, the molecular mechanisms that bring about this enhanced function and organization of IP_3R1 are unknown. In the present study, we considerably extend our previous findings (Jellerette et al., 2004) and demonstrate that during maturation and fertilization, IP_3R1 undergoes phosphorylation at a MPM2 epitope(s) in concert with the wax and wane of M-phase kinase activities in both mouse and *Xenopus* eggs and zygotes.

In mammals, where sperm-induced oscillations are long-lasting, other mechanisms besides the role of IP_3R1 have been proposed to account for the cell-cycle dependence of $[Ca^{2+}]_i$ oscillations (Carroll et al., 2004; Nixon et al., 2000; Nomikos et al., 2005), including the demonstration that PLCζ is sequestered away in the PN, presumably leading to reduced IP_3 production (Larman et al., 2004). Nonetheless, evidence in the literature shows that changes in the maternal Ca^{2+}-releasing machinery downstream of IP_3 production are also crucial for the association of Ca^{2+} release with M-phase stages in mammals and other species. For example, it has been shown that uninterrupted administration of IP_3 into PN-stage mouse zygotes does not restore oscillations (Jellerette et al., 2004; Jones and Whittingham, 1996). Likewise, in oscillating fertilized zygotes bisected after initiation of oscillations such that one half contains all nuclear structures, $[Ca^{2+}]_i$ oscillations cease at approximately the same time in both halves (Day et al., 2000). Lastly, cycling *Xenopus* egg extracts also show M-phase restricted IP_3R1-mediated Ca^{2+} release, regardless of whether cell-cycle resumption of the extracts was induced by the sperm or by a parthenogenetic agent (Tokmakov et al., 2001). Collectively, evidence suggests that the Ca^{2+}-releasing machinery of eggs undergoes a functional optimization during M-

phase stages of the cell cycle; we propose that MPM2 IP_3R1 phosphorylation is one of the mechanisms that underlie this optimization.

In this study, we have identified IP_3R1 as a novel target for MPM2-detectable phosphorylation during the M-phase stages of the cell cycle. The kinase(s) responsible for IP_3R1 phosphorylation in eggs is not yet known, although it is logical to envisage the participation of MPF and MAPK. Cdc2/cyclin B has already been shown to phosphorylate IP_3R1 in vitro and in vivo (Li et al., 2005; Malathi et al., 2003). In addition, substrate-binding motifs for this kinase were recently reported in IP_3Rs and, consistent with this, immunoprecipitation studies in breast cancer cells have shown that cyclins and IP_3R3 can interact (Soghoian et al., 2005). Despite this evidence, attempts to in vitro phosphorylate IP_3Rs using starfish oocyte extracts and recombinant Cdc2 kinase have produced negative results (Lim et al., 2003; Santella et al., 2003), which is consistent with our own unpublished results. The presumed role of MPF in MPM2 IP_3R1 reactivity is further undermined by our finding that the decline in MPM2 IP_3R1 reactivity and MPF activity during egg activation are not synchronous. Moreover, the preferred MPM2 epitope differs greatly from the preferred MPF phosphorylation motif (Holmes and Solomon, 1996). Nonetheless, it is still possible that MPF could actively phosphorylate IP_3R1 at a site undetectable by the MPM2 antibody. Future investigations should be pursued with more site-specific antibodies, such as those used by others (Malathi et al., 2003; Soghoian et al., 2005).

Our in vitro data reveal that MAPK phosphorylates IP_3R1 but not IP_3R3, and that this phosphorylation occurred within the domains that contain consensus sites for MAPK. Moreover, in vitro mutagenesis studies of the most-conserved site, S^{436}, showed that its substitution abolishes the phosphorylation of this domain by MAPK. Although mutation at a nearby conserved MPF site, S^{421}, decreased ERK-mediated phosphorylation within this GST-IP_3R1 fragment, it did not eliminate it. However, these results suggest that phosphorylation by one kinase may modify the effectiveness of phosphorylation by the second kinase, which is reminiscent of the effects observed after sequential phosphorylation of IP_3R1 by PKA and PKC (Vermassen et al., 2004a). Whether S^{436} is in vivo phosphorylated by MAPK/ERK and whether it becomes a MPM2 epitope require additional investigation. However, the recent demonstration in the peripheral Golgi protein Nir 2 that a S residue within a S^{382} PVE site, which is remarkably similar to the S^{436}PAE site in IP_3R1, becomes a MPM2 epitope at the onset of mitosis (Litvak et al., 2004) supports the concept that the S^{436} in IP_3R1 may also be actively modified during the MII stage.

Besides the previous demonstration in *Xenopus* egg extracts that MAPK/ERK was one of the kinases responsible for generating MPM2 reactivity sites (Kuang and Ashorn, 1993), our data showing that IP_3R1 MPM2 reactivity is not regained in Mit I zygotes, a stage that is devoid of MAPK activity, further implicates this pathway in playing a role in IP_3R1 phosphorylation. This association is further strengthened by the finding that MPM2 IP_3R1 reactivity was largely prevented in oocytes matured in the presence of the MEK inhibitor U0126. Moreover, ectopic activation of MAPK/ERK in PN-stage zygotes by the addition of OA re-established MPM2 reactivity. OA is known to promote PNBD by activating MAPK/ERK in the absence of MPF/Cdc2/cyclin B (Moos et al., 1995; Moos et al., 1996), although it is likely that other kinases are also activated by OA. Nevertheless, the OA-induced IP_3R1 phosphorylation was precluded by U0126, which supports the hypothesis that MAPK/ERK activity is required for IP_3R1 MPM2 phosphorylation. However, it is not possible to discern from these studies how MAPK/ERK brings about MPM2 IP_3R1 reactivity. For example, it could be by directly phosphorylating IP_3R1, which would support our in vitro studies. However, it is also feasible that ERK may activate other downstream kinases that are ultimately responsible for the phosphorylation. Given the pivotal role of MAPK/ERK in the cytoskeletal organization of the oocyte (Lefebvre et al., 2002; Verlhac et al., 2000), it is also plausible that this kinase could control the cellular distribution of IP_3R1 and the putative active kinase(s) such that they overlap at MII. Which of these possibilities, or what combination of them, underlies the role of MAPK/ERK on IP_3R1 MPM2 reactivity in eggs will require additional investigation.

Abrogation of the MAPK pathway and IP_3R1 MPM2 phosphorylation affected the oscillatory capacity of eggs. Our studies reveal that inhibition of IP_3R1 MPM2 reactivity by U0126 coincided with eggs showing $[Ca^{2+}]_i$ oscillations of shorter duration in response to $SrCl_2$ exposure or to PLCζ mRNA injection. In addition, the duration and amplitude of individual $[Ca^{2+}]_i$ rises were severely reduced in U0126-matured eggs. Importantly, the content of intracellular Ca^{2+} stores and the capacitative Ca^{2+} entry of these eggs appeared to be unaffected. Collectively, these results suggest that the oscillatory activity in general, and IP_3R1 function in particular, is compromised in eggs matured in the absence of the MAPK/ERK signaling pathway. A similar observation regarding the role of the MAPK pathway has been reported in sea urchin eggs, where abrogation of the MAPK signaling pathway prevented the $[Ca^{2+}]_i$ rise associated with nuclear-envelope breakdown and cell-cycle progression after fertilization (Philipova et al., 2005). These results differ, at least in part, from a recent publication that indicated that acute exposure of MII mouse eggs to U0126 was without consequences on sperm-initiated oscillations despite the reduction of MAPK/ERK activity (Marangos et al., 2003). However, whether or not the phosphorylation status of any of the downstream targets of MAPK/ERK was altered by the U0126 treatment, as demonstrated in our study for IP_3R1, was not determined in the aforementioned study.

In summary, we show that the IP_3R1 of vertebrate eggs is differentially phosphorylated at a MPM2 site(s) during oocyte maturation and after egg activation. We provide evidence that a M-phase kinase that phosphorylates IP_3R1 in vitro, MAPK/ERK, is required for the IP_3R1 MPM2-detectable in vivo phosphorylation observed in mouse eggs, and that elimination of the MPM2 reactivity may undermine the function of IP_3R1 during fertilization.

This work was supported by grants from the USDA and the NIH/NICHD to R.A.F.; and by grants G.0210.03 of the Fund for Scientific Research – Flanders, by P5/05 of the Interuniversity Attraction Poles Program of the Belgian Science Policy and by 04/07 of the Concerted Actions of the K.U.Leuven to H.D.S. and J.B.P. R.A.F. was a recipient of a visiting postdoctoral fellowship of the Fund for Scientific Research – Flanders. D.A. is supported by NIH grant DE016289. We also acknowledge the excellent technical assistance of I. Willems, L. Bauwens, S. Vangeel, T. Luyten and C. He, and comments on the manuscript by Dr Jeremy Smyth.

References

Araki, K., Naito, K., Haraguchi, S., Suzuki, R., Yokoyama, M., Inoue, M., Aizawa, S., Toyoda, Y. and Sato, E. (1996). Meiotic abnormalities of c-mos knockout mouse oocytes: activation after first meiosis or entrance into third meiotic metaphase. *Biol. Reprod.* **55**, 1315-1324.

Berridge, M. J. (2002). The endoplasmic reticulum: a multifunctional signaling organelle. *Cell Calcium* **32**, 235-249.

Berridge, M. J., Lipp, P. and Bootman, M. D. (2000). The versatility and universality of calcium signalling. *Nat. Rev. Mol. Cell Biol.* **1**, 11-21.

Bezprozvanny, I. (2005). The inositol 1,4,5-trisphosphate receptors. *Cell Calcium* **38**, 261-272.
Bosanac, I., Michikawa, T., Mikoshiba, K. and Ikura, M. (2004). Structural insights into the regulatory mechanism of IP3 receptor. *Biochim. Biophys. Acta* **1742**, 89-102.
Brind, S., Swann, K. and Carroll, J. (2000). Inositol 1,4,5-trisphosphate receptors are downregulated in mouse oocytes in response to sperm or adenophostin A but not to increases in intracellular Ca(2+) or egg activation. *Dev. Biol.* **223**, 251-265.
Bultynck, G., De Smet, P., Rossi, D., Callewaert, G., Missiaen, L., Sorrentino, V., De Smedt, H. and Parys, J. B. (2001). Characterization and mapping of the 12 kDa FK506-binding protein (FKBP12)-binding site on different isoforms of the ryanodine receptor and of the inositol 1,4,5-trisphosphate receptor. *Biochem. J.* **354**, 413-422.
Bultynck, G., Szlufcik, K., Kasri, N. N., Assefa, Z., Callewaert, G., Missiaen, L., Parys, J. B. and De Smedt, H. (2004). Thimerosal stimulates Ca2+ flux through inositol 1,4,5-trisphosphate receptor type 1, but not type 3, via modulation of an isoform-specific Ca2+-dependent intramolecular interaction. *Biochem. J.* **381**, 87-96.
Carroll, J. and Swann, K. (1992). Spontaneous cytosolic calcium oscillations driven by inositol trisphosphate occur during in vitro maturation of mouse oocytes. *J. Biol. Chem.* **267**, 11196-11201.
Carroll, J., FitzHarris, G., Marangos, P. and Halet, G. (2004). Ca2+ signalling and cortical re-organisation during the transition from meiosis to mitosis in mammalian oocytes. *Eur. J. Obstet. Gynecol. Reprod. Biol.* **115**, S61-S67.
Chatot, C. L., Ziomek, C. A., Bavister, B. D., Lewis, J. L. and Torres, I. (1989). An improved culture medium supports development of random-bred 1-cell mouse embryos in vitro. *J. Reprod. Fertil.* **86**, 679-688.
Che, S., Weil, M. M., Nelman-Gonzalez, M., Ashorn, C. L. and Kuang, J. (1997). MPM-2 epitope sequence is not sufficient for recognition and phosphorylation by ME kinase-H. *FEBS Lett.* **413**, 417-423.
Chiba, K., Kado, R. T. and Jaffe, L. A. (1990). Development of calcium release mechanisms during starfish oocyte maturation. *Dev. Biol.* **140**, 300-306.
Colledge, W. H., Carlton, M. B., Udy, G. B. and Evans, M. J. (1994). Disruption of c-mos causes parthenogenetic development of unfertilized mouse eggs. *Nature* **370**, 65-68.
Cousin, H., Gaultier, A., Bleux, C., Darribere, T. and Alfandari, D. (2000). PACSIN2 is a regulator of the metalloprotease/disintegrin ADAM13. *Dev. Biol.* **227**, 197-210.
Davis, F. M., Tsao, T. Y., Fowler, S. K. and Rao, P. N. (1983). Monoclonal antibodies to mitotic cells. *Proc. Natl. Acad. Sci. USA* **80**, 2926-2930.
Day, M. L., McGuinness, O. M., Berridge, M. J. and Johnson, M. H. (2000). Regulation of fertilization-induced Ca(2+)spiking in the mouse zygote. *Cell Calcium* **28**, 47-54.
Ding, M., Feng, Y. and Vandre, D. D. (1997). Partial characterization of the MPM-2 phosphoepitope. *Exp. Cell Res.* **231**, 3-13.
Ducibella, T., Huneau, D., Angelichio, E., Xu, Z., Schultz, R. M., Kopf, G. S., Fissore, R., Madoux, S. and Ozil, J. P. (2002). Egg-to-embryo transition is driven by differential responses to Ca(2+) oscillation number. *Dev. Biol.* **250**, 280-291.
Favata, M. F., Horiuchi, K. Y., Manos, E. J., Daulerio, A. J., Stradley, D. A., Feeser, W. S., Van Dyk, D. E., Pitts, W. J., Earl, R. A., Hobbs, F. et al. (1998). Identification of a novel inhibitor of mitogen-activated protein kinase kinase. *J. Biol. Chem.* **273**, 18623-18632.
Ferris, C. D., Huganir, R. L., Bredt, D. S., Cameron, A. M. and Snyder, S. H. (1991). Inositol trisphosphate receptor: phosphorylation by protein kinase C and calcium calmodulin-dependent protein kinases in reconstituted lipid vesicles. *Proc. Natl. Acad. Sci. USA* **88**, 2232-2235.
FitzHarris, G., Marangos, P. and Carroll, J. (2003). Cell cycle-dependent regulation of structure of endoplasmic reticulum and inositol 1,4,5-Trisphosphate-induced Ca(2+) release in mouse oocytes and embryos. *Mol. Biol. Cell* **14**, 288-301.
Fujiwara, T., Nakada, K., Shirakawa, H. and Miyazaki, S. (1993). Development of inositol trisphosphate-induced calcium release mechanism during maturation of hamster oocytes. *Dev. Biol.* **156**, 69-79.
Gordo, A. C., Kurokawa, M., Wu, H. and Fissore, R. A. (2002). Modifications of the Ca2+ release mechanisms of mouse oocytes by fertilization and by sperm factor. *Mol. Hum. Reprod.* **8**, 619-629.
Goud, P. T., Goud, A. P., Van Oostveldt, P. and Dhont, M. (1999). Presence and dynamic redistribution of type I inositol 1,4,5-trisphosphate receptors in human oocytes and embryos during in-vitro maturation, fertilization and early cleavage divisions. *Mol. Hum. Reprod.* **5**, 441-451.
Halet, G., Tunwell, R., Parkinson, S. J. and Carroll, J. (2004). Conventional PKCs regulate the temporal pattern of Ca2+ oscillations at fertilization in mouse eggs. *J. Cell Biol.* **164**, 1033-1044.
Hashimoto, N., Watanabe, N., Furuta, Y., Tamemoto, H., Sagata, N., Yokoyama, M., Okazaki, K., Nagayoshi, M., Takeda, N., Ikawa, Y. et al. (1994). Parthenogenetic activation of oocytes in c-mos-deficient mice. *Nature* **370**, 68-71.
He, C. L., Damiani, P., Ducibella, T., Takahashi, M., Tanzawa, K., Parys, J. B. and Fissore, R. A. (1999). Isoforms of the inositol 1,4,5-trisphosphate receptor are expressed in bovine oocytes and ovaries: the type-1 isoform is down-regulated by fertilization and by injection of adenophostin A. *Biol. Reprod.* **61**, 935-943.
Holmes, J. K. and Solomon, M. J. (1996). A predictive scale for evaluating cyclin-dependent kinase substrates. A comparison of p34cdc2 and p33cdk2. *J. Biol. Chem.* **271**, 25240-25246.
Iwasaki, H., Chiba, K., Uchiyama, T., Yoshikawa, F., Suzuki, F., Ikeda, M., Furuichi, T. and Mikoshiba, K. (2002). Molecular characterization of the starfish inositol 1,4,5-trisphosphate receptor and its role during oocyte maturation and fertilization. *J. Biol. Chem.* **277**, 2763-2772.
Jayaraman, T., Ondrias, K., Ondriasova, E. and Marks, A. R. (1996). Regulation of the inositol 1,4,5-trisphosphate receptor by tyrosine phosphorylation. *Science* **272**, 1492-1494.
Jellerette, T., He, C. L., Wu, H., Parys, J. B. and Fissore, R. A. (2000). Down-regulation of the inositol 1,4,5-trisphosphate receptor in mouse eggs following fertilization or parthenogenetic activation. *Dev. Biol.* **223**, 238-250.
Jellerette, T., Kurokawa, M., Lee, B., Malcuit, C., Yoon, S.-Y., Smyth, J., Vermassen, E., De Smedt, H., Parys, J. B. and Fissore, R. A. (2004). Cell cycle-coupled [Ca2+]i oscillations in mouse zygotes and function of the inositol 1,4,5-trisphosphate receptor-1. *Dev. Biol.* **274**, 94-109.
Jones, K. T. and Whittingham, D. G. (1996). A comparison of sperm- and IP3-induced Ca2+ release in activated and aging mouse oocytes. *Dev. Biol.* **178**, 229-237.
Jones, K. T., Carroll, J., Merriman, J. A., Whittingham, D. G. and Kono, T. (1995). Repetitive sperm-induced Ca2+ transients in mouse oocytes are cell cycle dependent. *Development* **121**, 3259-3266.
Khan, M. T., Wagner, L., 2nd, Yule, D. I., Bhanumathy, C. and Joseph, S. K. (2006). Akt kinase phosphorylation of inositol 1,4,5-trisphosphate receptors. *J. Biol. Chem.* **281**, 3731-3737.
Kline, D. and Kline, J. (1992a). Repetitive calcium transients and the role of calcium in exocytosis and cell cycle activation in the mouse egg. *Dev. Biol.* **149**, 80-89.
Kline, D. and Kline, J. (1992b). Thapsigargin activates a calcium influx pathway in the unfertilized mouse egg and suppresses repetitive calcium transients in the fertilized egg. *J. Biol. Chem.* **267**, 17624-17630.
Kline, D., Mehlmann, L., Fox, C. and Terasaki, M. (1999). The cortical endoplasmic reticulum (ER) of the mouse egg: localization of ER clusters in relation to the generation of repetitive calcium waves. *Dev. Biol.* **215**, 431-442.
Koga, T., Yoshida, Y., Cai, J. Q., Islam, M. O. and Imai, S. (1994). Purification and characterization of 240-kDa cGMP-dependent protein kinase substrate of vascular smooth muscle. Close resemblance to inositol 1,4,5-trisphosphate receptor. *J. Biol. Chem.* **269**, 11640-11647.
Kono, T., Jones, K. T., Bos-Mikich, A., Whittingham, D. G. and Carroll, J. (1996). A cell cycle-associated change in Ca2+ releasing activity leads to the generation of Ca2+ transients in mouse embryos during the first mitotic division. *J. Cell Biol.* **132**, 915-923.
Kouchi, Z., Fukami, K., Shikano, T., Oda, S., Nakamura, Y., Takenawa, T. and Miyazaki, S. (2004). Recombinant phospholipase Czeta has high Ca2+ sensitivity and induces Ca2+ oscillations in mouse eggs. *J. Biol. Chem.* **279**, 10408-10412.
Kuang, J. and Ashorn, C. L. (1993). At least two kinases phosphorylate the MPM-2 epitope during Xenopus oocyte maturation. *J. Cell Biol.* **123**, 859-868.
Kume, S., Muto, A., Aruga, J., Nakagawa, T., Michikawa, T., Furuichi, T., Nakade, S., Okano, H. and Mikoshiba, K. (1993). The Xenopus IP3 receptor: structure, function, and localization in oocytes and eggs. *Cell* **73**, 555-570.
Kurokawa, M., Sato, K., Smyth, J., Wu, H., Fukami, K., Takenawa, T. and Fissore, R. A. (2004). Evidence that activation of Src family kinase is not required for fertilization-associated [Ca2+]i oscillations in mouse eggs. *Reproduction* **127**, 441-454.
Kurokawa, M., Sato, K., Wu, H., He, C., Malcuit, C., Black, S. J., Fukami, K. and Fissore, R. A. (2005). Functional, biochemical, and chromatographic characterization of the complete [Ca(2+)](i) oscillation-inducing activity of porcine sperm. *Dev. Biol.* **285**, 376-392.
Laemmli, U. K. (1970). Cleavage of structural proteins during the assembly of the head of bacteriophage T4. *Nature* **227**, 680-685.
Larman, M. G., Saunders, C. M., Carroll, J., Lai, F. A. and Swann, K. (2004). Cell cycle-dependent Ca2+ oscillations in mouse embryos are regulated by nuclear targeting of PLCzeta. *J. Cell Sci.* **117**, 2513-2521.
Lefebvre, C., Terret, M. E., Djiane, A., Rassinier, P., Maro, B. and Verlhac, M. H. (2002). Meiotic spindle stability depends on MAPK-interacting and spindle-stabilizing protein (MISS), a new MAPK substrate. *J. Cell Biol.* **157**, 603-613.
Li, X., Malathi, K., Krizanova, O., Ondrias, K., Sperber, K., Ablamunits, V. and Jayaraman, T. (2005). Cdc2/Cyclin B1 interacts with and modulates inositol 1,4,5-Trisphosphate receptor (Type 1) functions. *J. Immunol.* **175**, 6205-6210.
Lim, D., Ercolano, E., Kyozuka, K., Nusco, G. A., Moccia, F., Lange, K. and Santella, L. (2003). The M-phase-promoting factor modulates the sensitivity of the Ca2+ stores to inositol 1,4,5-trisphosphate via the actin cytoskeleton. *J. Biol. Chem.* **278**, 42505-42514.

Litvak, V., Argov, R., Dahan, N., Ramachandran, S., Amarilio, R., Shainskaya, A. and Lev, S. (2004). Mitotic phosphorylation of the peripheral golgi protein Nir2 by Cdk1 provides a docking mechanism for Plk1 and affects cytokinesis completion. *Mol. Cell* **14**, 319-330.
Malathi, K., Kohyama, S., Ho, M., Soghoian, D., Li, X., Silane, M., Berenstein, A. and Jayaraman, T. (2003). Inositol 1,4,5-trisphosphate receptor (type 1) phosphorylation and modulation by Cdc2. *J. Cell Biochem.* **90**, 1186-1196.
Marangos, P., FitzHarris, G. and Carroll, J. (2003). Ca2+ oscillations at fertilization in mammals are regulated by the formation of pronuclei. *Development* **130**, 1461-1472.
Masui, Y. and Markert, C. L. (1971). Cytoplasmic control of nuclear behavior during meiotic maturation of frog oocytes. *J. Exp. Zool.* **177**, 129-145.
McDougall, A. and Levasseur, M. (1998). Sperm-triggered calcium oscillations during meiosis in ascidian oocytes first pause, restart, then stop: correlations with cell cycle kinase activity. *Development* **125**, 4451-4459.
Mehlmann, L. M. and Kline, D. (1994). Regulation of intracellular calcium in the mouse egg: calcium release in response to sperm or inositol trisphosphate is enhanced after meiotic maturation. *Biol. Reprod.* **51**, 1088-1098.
Meijer, L., Borgne, A., Mulner, O., Chong, J. P., Blow, J. J., Inagaki, N., Inagaki, M., Delcros, J. G. and Moulinoux, J. P. (1997). Biochemical and cellular effects of roscovitine, a potent and selective inhibitor of the cyclin-dependent kinases cdc2, cdk2 and cdk5. *Eur. J. Biochem.* **243**, 527-536.
Miyazaki, S., Yuzaki, M., Nakada, K., Shirakawa, H., Nakanishi, S., Nakade, S. and Mikoshiba, K. (1992). Block of Ca2+ wave and Ca2+ oscillation by antibody to the inositol 1,4,5-trisphosphate receptor in fertilized hamster eggs. *Science* **257**, 251-255.
Miyazaki, S., Shirakawa, H., Nakada, K. and Honda, Y. (1993). Essential role of the inositol 1,4,5-trisphosphate receptor/Ca2+ release channel in Ca2+ waves and Ca2+ oscillations at fertilization of mammalian eggs. *Dev. Biol.* **158**, 62-78.
Moos, J., Visconti, P. E., Moore, G. D., Schultz, R. M. and Kopf, G. S. (1995). Potential role of mitogen-activated protein kinase in pronuclear envelope assembly and disassembly following fertilization of mouse eggs. *Biol. Reprod.* **53**, 692-699.
Moos, J., Xu, Z., Schultz, R. M. and Kopf, G. S. (1996). Regulation of nuclear envelope assembly/disassembly by MAP kinase. *Dev. Biol.* **175**, 358-361.
Nigg, E. A. (1991). The substrates of the cdc2 kinase. *Semin. Cell Biol.* **2**, 261-270.
Nixon, V. L., McDougall, A. and Jones, K. T. (2000). Ca2+ oscillations and the cell cycle at fertilisation of mammalian and ascidian eggs. *Biol. Cell* **92**, 187-196.
Nomikos, M., Blayney, L. M., Larman, M. G., Campbell, K., Rossbach, A., Saunders, C. M., Swann, K. and Lai, F. A. (2005). Role of phospholipase C-zeta domains in Ca2+-dependent phosphatidylinositol 4,5-bisphosphate hydrolysis and cytoplasmic Ca2+ oscillations. *J. Biol. Chem.* **280**, 31011-31018.
Parrington, J., Brind, S., De Smedt, H., Gangeswaran, R., Lai, F. A., Wojcikiewicz, R. and Carroll, J. (1998). Expression of inositol 1,4,5-trisphosphate receptors in mouse oocytes and early embryos: the type I isoform is upregulated in oocytes and downregulated after fertilization. *Dev. Biol.* **203**, 451-461.
Parys, J. B., Sernett, S. W., DeLisle, S., Snyder, P. M., Welsh, M. J. and Campbell, K. P. (1992). Isolation, characterization, and localization of the inositol 1,4,5-trisphosphate receptor protein in Xenopus laevis oocytes. *J. Biol. Chem.* **267**, 18776-18782.
Parys, J. B., De Smedt, H., Missiaen, L., Bootman, M. D., Sienaert, I. and Casteels, R. (1995). Rat basophilic leukemia cells as model system for inositol 1,4,5-trisphosphate receptor IV, a receptor of the type II family: functional comparison and immunological detection. *Cell Calcium* **17**, 239-249.
Patel, S., Joseph, S. K. and Thomas, A. P. (1999). Molecular properties of inositol 1,4,5-trisphosphate receptors. *Cell Calcium* **25**, 247-264.
Patterson, R. L., Boehning, D. and Snyder, S. H. (2004a). Inositol 1,4,5-trisphosphate receptors as signal integrators. *Annu. Rev. Biochem.* **73**, 437-465.
Patterson, R. L., van Rossum, D. B., Barrow, R. K. and Snyder, S. H. (2004b). RACK1 binds to inositol 1,4,5-trisphosphate receptors and mediates Ca2+ release. *Proc. Natl. Acad. Sci. USA* **101**, 2328-2332.
Philipova, R., Kisielewska, J., Lu, P., Larman, M., Huang, J. Y. and Whitaker, M. (2005). ERK1 activation is required for S-phase onset and cell cycle progression after fertilization in sea urchin embryos. *Development* **132**, 579-589.
Phillips, K. P., Petrunewich, M. A., Collins, J. L., Booth, R. A., Liu, X. J. and Baltz, J. M. (2002). Inhibition of MEK or cdc2 kinase parthenogenetically activates mouse eggs and yields the same phenotypes as Mos(–/–) parthenogenotes. *Dev. Biol.* **247**, 210-223.
Runft, L. L., Watras, J. and Jaffe, L. A. (1999). Calcium release at fertilization of Xenopus eggs requires type I IP(3) receptors, but not SH2 domain-mediated activation of PLCgamma or G(q)-mediated activation of PLCbeta. *Dev. Biol.* **214**, 399-411.
Santella, L., Ercolano, E., Lim, D., Nusco, G. A. and Moccia, F. (2003). Activated M-phase-promoting factor (MPF) is exported from the nucleus of starfish oocytes to increase the sensitivity of the Ins(1,4,5)P3 receptors. *Biochem. Soc. Trans.* **31**, 79-82.
Saunders, C. M., Larman, M. G., Parrington, J., Cox, L. J., Royse, J., Blayney, L. M., Swann, K. and Lai, F. A. (2002). PLC zeta: a sperm-specific trigger of Ca(2+) oscillations in eggs and embryo development. *Development* **129**, 3533-3544.
Schultz, R. M. and Kopf, G. S. (1995). Molecular basis of mammalian egg activation. *Curr. Trends Dev. Biol.* **30**, 21-62.
Shuttleworth, T. J. and Thompson, J. L. (1992). Modulation of inositol(1,4,5)trisphosphate-sensitive calcium store content during continuous receptor activation and its effects on calcium entry. *Cell Calcium* **13**, 541-551.
Singleton, P. A. and Bourguignon, L. Y. (2002). CD44v10 interaction with Rho-kinase (ROK) activates inositol 1,4,5-triphosphate (IP3) receptor-mediated Ca2+ signaling during hyaluronan (HA)-induced endothelial cell migration. *Cell Motil. Cytoskeleton* **53**, 293-316.
Sipma, H., De Smet, P., Sienaert, I., Vanlingen, S., Missiaen, L., Parys, J. B. and De Smedt, H. (1999). Modulation of inositol 1,4,5-trisphosphate binding to the recombinant ligand-binding site of the type-1 inositol 1,4, 5-trisphosphate receptor by Ca2+ and calmodulin. *J. Biol. Chem.* **274**, 12157-12162.
Smyth, J. T., Abbott, A. L., Lee, B., Sienaert, I., Kasri, N. N., De Smedt, H., Ducibella, T., Missiaen, L., Parys, J. B. and Fissore, R. A. (2002). Inhibition of the inositol trisphosphate receptor of mouse eggs and A7r5 cells by KN-93 via a mechanism unrelated to Ca2+/calmodulin-dependent protein kinase II antagonism. *J. Biol. Chem.* **277**, 35061-35070.
Soghoian, D., Jayaraman, V., Silane, M., Berenstein, A. and Jayaraman, T. (2005). Inositol 1,4,5-trisphosphate receptor phosphorylation in breast cancer. *Tumour Biol.* **26**, 207-212.
Stith, B. J., Goalstone, M., Silva, S. and Jaynes, C. (1993). Inositol 1,4,5-trisphosphate mass changes from fertilization through first cleavage in Xenopus laevis. *Mol. Biol. Cell* **4**, 435-443.
Stricker, S. A. (1999). Comparative biology of calcium signaling during fertilization and egg activation in animals. *Dev. Biol.* **211**, 157-176.
Stricker, S. A. and Smythe, T. L. (2003). Endoplasmic reticulum reorganizations and Ca2+ signaling in maturing and fertilized oocytes of marine protostome worms: the roles of MAPKs and MPF. *Development* **130**, 2867-2879.
Swann, K., Igusa, Y. and Miyazaki, S. (1989). Evidence for an inhibitory effect of protein kinase C on G-protein-mediated repetitive calcium transients in hamster eggs. *EMBO J.* **8**, 3711-3718.
Thastrup, O., Cullen, P. J., Drobak, B. K., Hanley, M. R. and Dawson, A. P. (1990). Thapsigargin, a tumor promoter, discharges intracellular Ca2+ stores by specific inhibition of the endoplasmic reticulum Ca2(+)-ATPase. *Proc. Natl. Acad. Sci. USA* **87**, 2466-2470.
Tokmakov, A. A., Sato, K. I. and Fukami, Y. (2001). Calcium oscillations in Xenopus egg cycling extracts. *J. Cell Biochem.* **82**, 89-97.
Turner, P. R., Sheetz, M. P. and Jaffe, L. A. (1984). Fertilization increases the polyphosphoinositide content of sea urchin eggs. *Nature* **310**, 414-415.
Verlhac, M. H., Lefebvre, C., Guillaud, P., Rassinier, P. and Maro, B. (2000). Asymmetric division in mouse oocytes: with or without Mos. *Curr. Biol.* **10**, 1303-1306.
Vermassen, E., Fissore, R. A., Nadif Kasri, N., Vanderheyden, V., Callewaert, G., Missiaen, L., Parys, J. B. and De Smedt, H. (2004a). Regulation of the phosphorylation of the inositol 1,4,5-trisphosphate receptor by protein kinase C. *Biochem. Biophys. Res. Commun.* **319**, 888-893.
Vermassen, E., Parys, J. B. and Mauger, J. P. (2004b). Subcellular distribution of the inositol 1,4,5-trisphosphate receptors: functional relevance and molecular determinants. *Biol. Cell* **96**, 3-17.
Westendorf, J., Rao, P. and Gerace, L. (1994). Cloning of cDNAs for M-Phase phosphoproteins recognized by the MPM2 monoclonal antibody and determination of the phosphorylated epitope. *Proc. Natl. Acad. Sci. USA* **91**, 714-718.
Whitaker, M. (2006). Calcium at fertilization and in early development. *Physiol. Rev.* **86**, 25-88.
Whitaker, M. and Patel, R. (1990). Calcium and cell cycle control. *Development* **108**, 525-542.
Winston, N., McGuinness, O., Johnson, M. and Maro, B. (1995). The exit of mouse oocytes from meiotic M-phase requires an intact spindle during intracellular calcium release. *J. Cell Sci.* **108**, 143-151.
Yokoyama, K., Su, I., Tezuka, T., Yasuda, T., Mikoshiba, K., Tarakhovsky, A. and Yamamoto, T. (2002). BANK regulates BCR-induced calcium mobilization by promoting tyrosine phosphorylation of IP(3) receptor. *EMBO J.* **21**, 83-92.
Yoshikawa, F., Iwasaki, H., Michikawa, T., Furuichi, T. and Mikoshiba, K. (1999). Trypsinized cerebellar inositol 1,4,5-trisphosphate receptor. Structural and functional coupling of cleaved ligand binding and channel domains. *J. Biol. Chem.* **274**, 316-327.
Zhu, D. M., Tekle, E., Chock, P. B. and Huang, C. Y. (1996). Reversible phosphorylation as a controlling factor for sustaining calcium oscillations in HeLa cells: Involvement of calmodulin-dependent kinase II and a calyculin A-inhibitable phosphatase. *Biochemistry* **35**, 7214-7223.